Long Distance Wave Propagation Through Rain at High Millimeter-Wave Frequencies

Adib Y. Nashashibi[1] and Kamal Sarabandi[1]*

[1]Radiation Laboratory, Department of Electrical Engineering and Computer Science, University of Michigan, Ann Arbor, MI 48109-2122, USA (email: nuha@umich.edu, saraband@umich.edu).

Abstract

Monte Carlo simulations are performed numerically to characterize the behavior of both the forward and backward scattered fields for a millimeter source different rain media. Especial attention is given to long-distance wave propagation in such media. Numerical simulations are performed at high millimeter-wave frequencies using distorted Born approximation in conjunction with single scattering for rain droplets for a narrow beam radar whereby both the radar within the rain medium.

1. Introduction

The ability to design compact and lightweight millimeter-wave (MMW) radars has led to a proliferation of radars at such frequencies for a wide range of applications, such as collision avoidance, assistive landing of airborne vehicles, high-resolution synthetic aperture radar imaging, and autonomous navigation of robotic ground and air vehicles[1,3]. At high millimeter-wave frequencies (90 GHz < f < 300 GHz), wave propagation through the atmosphere is of concern, especially during inclement weather. Distortions introduced by rain, in the form of extinction, depolarization, and increased backscatter, are of particular concern due to the fact that water droplets have a higher permittivity and larger size than other airborne particles. The size of a water droplet may extend anywhere between few microns and 8 mm in diameter. At 94 GHz, for example, where the wavelength is 3.2 mm, a significant number of the rain droplets may be considered as electrically large particles with strong scattering and extinction. Few well-designed experiments aimed at characterizing the rain extinction and backscattering at MMW frequencies have been reported in open literature [4-8]. These reported measurements were conducted over relatively short distances. Figure 1 compares between the measured attenuation rates and reflectivity of rain at different rainfall rates and theoretical predictions assuming different particle size distribution models [6].

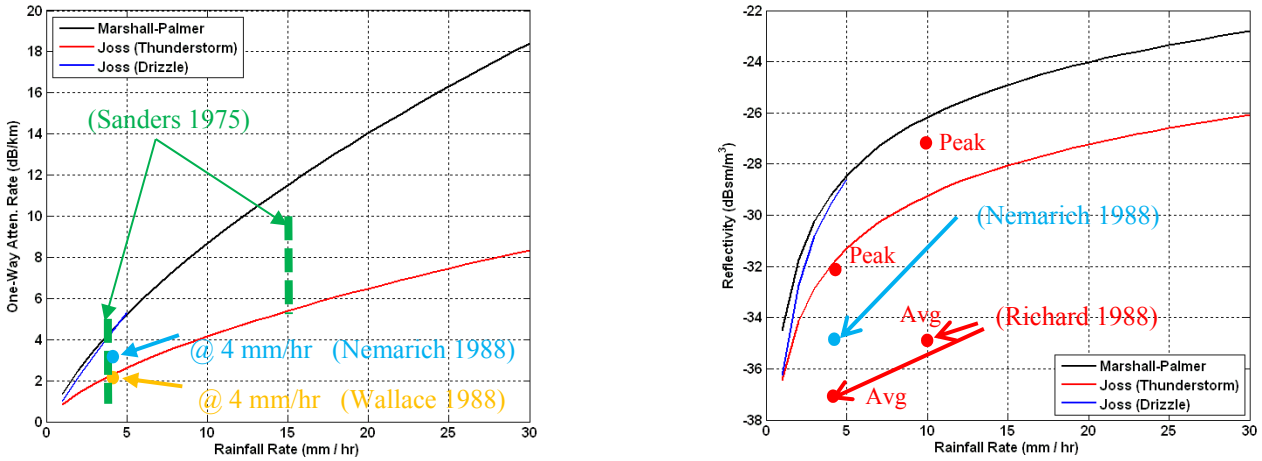

(a) Attenuation rate (b) Reflectivity

Figure 1: Comparison between measurements and theoretically calculated (a) one-way attenuation rates and (b) reflectivity of rain as function of rainfall rate. Different particle size distribution models have been considered.

However, the impact of MMW signal propagation through the rain medium over long distances has not been studied adequately, specifically, in terms of (a) extinction rate, (b) depolarization, and (c) amplitude and phase distortions of the wave front. The expectation is that over long distances and under heavy rain conditions, the mean incident field diminishes while the incoherent forward-scattered field increases leading to a change in extinction rate. The presence of non-spherical large rain droplets in the path of the radar signal may generate cross-polarized response in both the forward and backward directions resulting in polarization signature distortions of targets, which may hamper detection algorithms that are based on cross-polarized response. Furthermore, accumulative effects of the scattered fields in the forward direction may lead to significant distortions in amplitude and phase of the signal's wave front (aberrations) which can lead to errors in range

978-1-4673-5225-3/14/$31.00 ©2014 IEEE

determinations and degradation in radar images. In this paper, we present Monte-Carlo type numerical simulations of the propagating wave through homogeneous rain medium. The simulations are based on single scattering and Foldy's approximation. In addition, both the target and the radar locations are assumed to be within the rain medium and the propagating wave is bound by the radar's antenna pattern.

2. Numerical Simulations

In the proposed simulations, it is assumed that (a) the transmit antenna is narrow with beamwidth β_{max}, (b) the rain medium is a uniformly distributed (this uniformity is in 3-D), and (c) the observation point (target location) is at a long distance R_o away from the transmitter. The contribution to the total scattered field in both directions is from droplets that are within the conical volume as depicted in Fig. 2. The governing equations of the scattered fields in both the forward and backward directions can be derived from the radar equation. In the forward direction case, the total propagating field is calculated at the point (distance) of interest by coherently adding the forward scattered fields of all rain droplets in the signal path. The scattered field from the nth particle within the signal path is given by:

$$E_f^n = \sqrt{P_t G(\theta_n,\varphi_n)}\sqrt{\frac{1}{4\pi R_{tn}^2}}s_n e^{-(\alpha-ik)(R_{tn}+R_{nr})}\sqrt{\frac{1}{4\pi R_{nr}^2}} = \frac{\sqrt{P_t G_n}}{4\pi}\frac{s_n}{R_{tn}R_{nr}}e^{-(\alpha-ik)(R_{tn}+R_{nr})} \quad (1)$$

where α is the attenuation rate (one-way) in Np/m, s_n is the complex scattering amplitude of the nth droplet, P_t is the transmitted power (can be normalized to 1 without loss of generality), $G(\theta_n,\phi_n)$ is the antenna gain along direction defined by angles θ_n and ϕ_n, k is the wavenumber in free space, R_{nr} and R_{tn} are the distances from the nth particle to the receiving point and the transmitter, respectively. The total received field (forward direction) includes both the direct path field and the total scattered field from all raindrops and is given by:

$$E_f = \sum_n\left[\frac{\sqrt{P_t G_n}}{4\pi}\frac{s_n}{R_{tn}R_{nr}}e^{-(\alpha-ik)(R_{tn}+R_{nr})}\right] + \sqrt{\frac{P_t G_{max}}{4\pi}}\frac{e^{-(\alpha-ik)R_o}}{R_o} \quad (2)$$

Similar expressions can be derived in the backward direction (radar return) that includes the receive antenna (which is assumed to be identical to the transmit antenna).

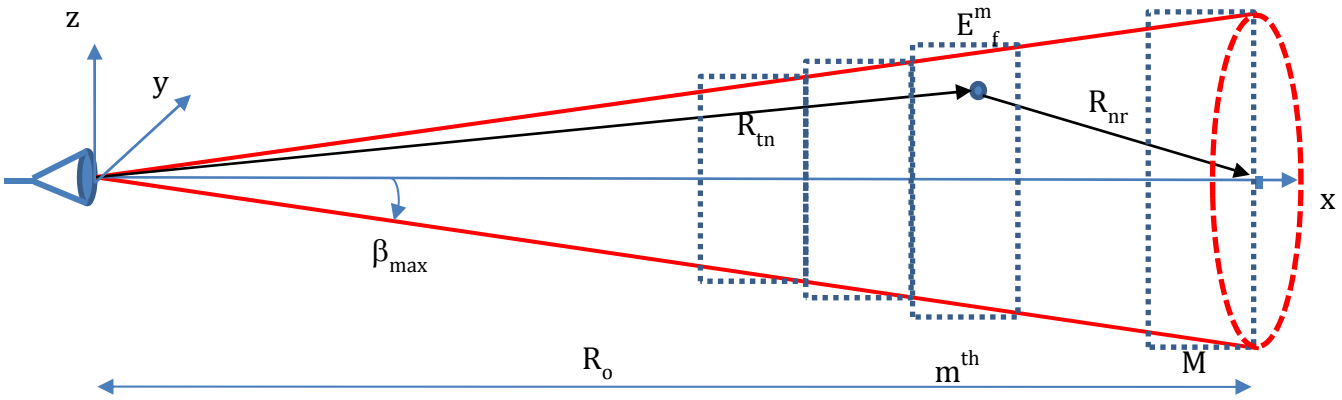

Figure 2: Narrow beam radar illumination of the uniformly distributed rain medium.

Consistent with the uniformity assumption in the rain medium, random locations of the water droplets are generated within the conical illuminated 3-D volume (Fig. 2). The particle size at any of these random locations is randomly selected according to the particle size distribution function being used, which in turn is a function of the rainfall rate. Different particle size distributions have been proposed in the open literature [6]. Here we have selected the Marshall-Palmer distribution function. To simplify the calculations and permit the isolation of returns from different range-bins, the propagation path can be divided into M-sections. For each section the random locations of particles are checked to determine if they are within the antenna beam, otherwise they are dropped. For the accepted locations, size particles are generated according to the Marshall-Palmer particle size distribution function. The total forward and backward scattered fields are calculated at each range-bin (i.e. section) and stored separately. For example, consider the case of a 94 GHz radar using a narrow beam antenna of 1° beamwidth and 45 dBi in gain, illuminating a uniformly distributed rain medium with a rainfall rate of 2 mm/hr (light rain) and one-way attenuation rate of 2 dB/km. For this example, over 100 Monte Carlo simulations were performed and the forward scattered fields were collected for up to 1000 m away from the radar. The forward scattered field due to the

individual range-bins (1 m wide in this example) that is received at the maximum range is plotted in Fig. 3a as function of the range-bin distance. It is clear that the dominant contribution is expected to occur when the water droplets are closer to the observation point. Nevertheless, the further away range-bins do contribute to the total field at the observation point, as shown in Fig. 3b (here all scattered fields from different range-bins are added coherently). In this particular example, the direct (or incident) coherent field propagating through the rain medium and suffering from attenuation is still dominant. At the conference time, it will be shown that at longer distances and higher rainfall rates (where the number of rain droplets and size increase significantly), the power of the incoherent component will exceed that of the coherent field.

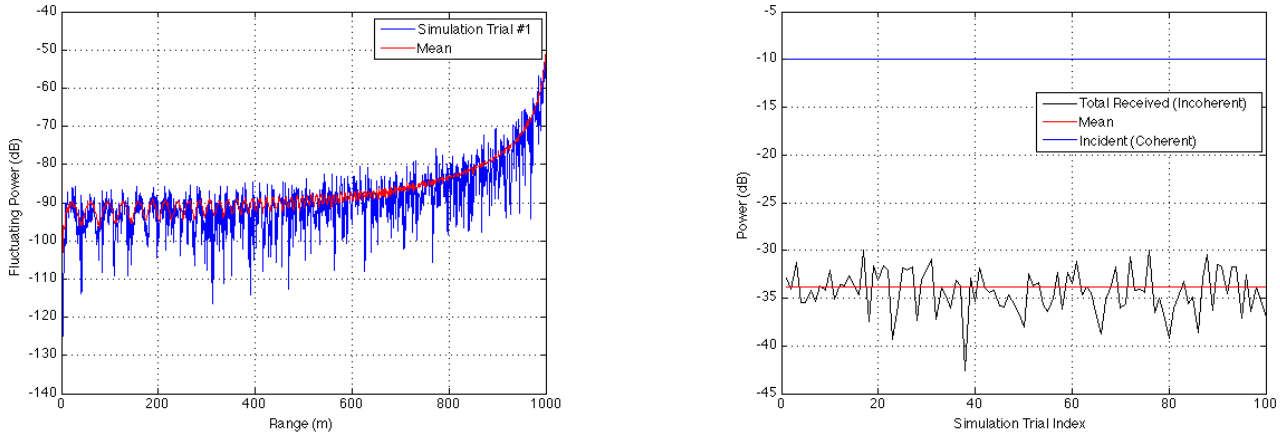

(a) (b)

Figure 3: Simulated forward scattered field of light rainfall rate (2 mm/hr) (a) at 94 GHz when illuminated with narrow beam. In (a) the forward scattered field from individual range-bins that is received at the observation point (1000 m) is plotted a function of the range-bin location and (b) the total forward field is plotted a function of simulation trial index

It is thought that groups of particles within the beam may not contribute significantly to the total forward scattered field, so they can be ignored and the Monte Carlo simulations can be accelerated further. The criterion to whether or not ignore the contribution of a region/group of particles is the relative strength of its field compared to the direct field propagating through the random medium. This can be expressed as the ratio between the forward scattered field from the region of interest to the direct field. The field equation described above includes deterministic quantities, such as the range to and from the particle, the antenna gain, and the attenuation rate. It also includes random quantities that depend on the raindrop size and shape. Consider the following ratio:

$$\frac{E_f}{E_d} = \frac{\dfrac{e^{-\alpha(R_1+R_2)}\sqrt{g(\theta)G_{\max}}}{R_1 R_2}}{\dfrac{e^{-\alpha R_o}\sqrt{G_{\max}}}{R_o}} = C \tag{3}$$

where C is a constant, $g(\theta)$ is the antenna gain at off-axis angle θ, G_{max} is maximum antenna gain, and R_1 and R_2 refer to the distances between the particle and the radar and observation point respectively. The value of this ratio changes as function of particle coordinates (x, y) within the beam, irrespective of the particle's size, shape, and orientation. One can generate contours that describe the coordinates of points that have the same ratio. An example of contour plot of constant ratio is shown in Fig. 4. In this example, the antenna had 1^o beamwidth, observation point is located at 10 km, and the rain attenuation rate is set to 2 dB/km (light rain case). The figure clearly demonstrates that only a fraction of the illuminated volume needs to be considered for simulating the forward scattered field.

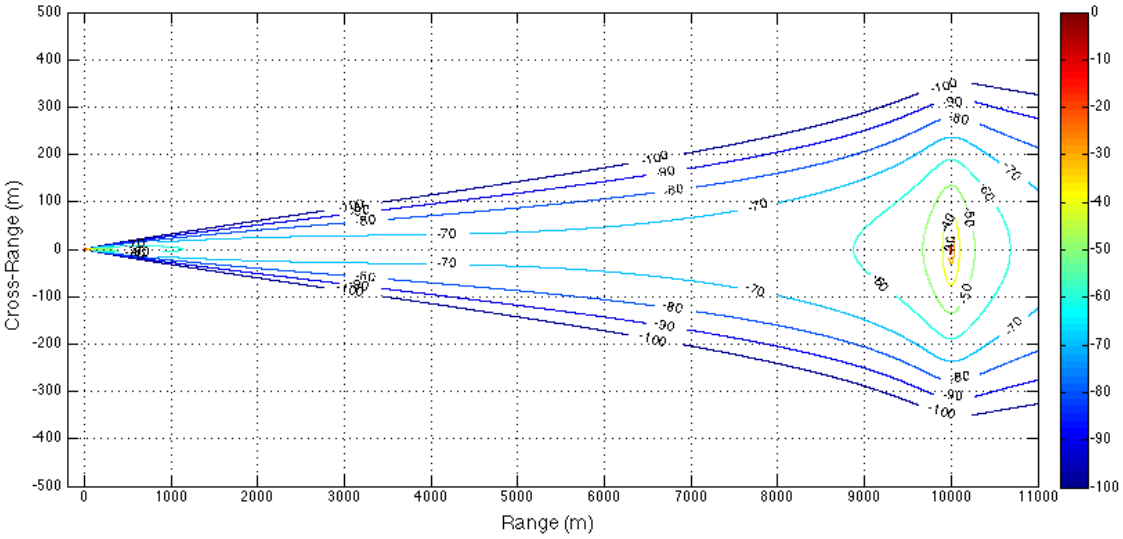

Figure 4: Contours of the ratio between the forward scattered field and direct (incident) field assuming that the radar's beamwidth is 1°, the observation point is at 10 km away, and the rain attenuation rate is 2 dB/km. Only geometric parameters are considered in generating the contours.

3. Conclusion

Millimeter-wave signals propagating through rain may suffer from significant amplitude and phase distortions over long propagation distances, especially at high rainfall rates where the number of droplets per unit volume increase dramatically as well as the percentage of large droplets to the total number of particles. Under certain conditions, the forward scattered field may exceed in strength the direct incident field and in effect drive the value of the extinction rate through the rain medium.

4. References

[1] M. Rangwala, F. Wang, and K. Sarabandi, "Study of Millimeter-Wave Radar for Helicopter Assisted Landing System," IEEE AP Magazine, pp. 13 – 25, Vol. 50, Issue 2, April 2008.

[2] Sarabandi, K., Eric S. Li, and A. Nashashibi, "Modeling and Measurements of Scattering from Road Surfaces at Millimeter-Wave Frequencies," IEEE Trans. AP, vol. 45, no. 11, pp. 1679-1688, November 1997.

[3] Moallem, M., and K. Sarabandi, "Y-Band Radar Assessment for Indoor Navigation and Mapping, USNC-URSI National Radio Science, Boulder, Colorado, 8-12 Jan. 2013.

[4] H. B. Wallace, "Millimeter-wave propagation measurements at the ballistic research laboratory," *IEEE TGRS*, vol. 26, no. 3, pp. 253-258, May 1988.

[5] V. W. Richard, J. E. Kammerer, and H. B. Wallace, "Rain backscatter measurements at millimeter wavelengths," *IEEE Transactions on Geoscience and Remote Sensing*, vol. 26, no. 3, pp. 244-252, May 1988.

[6] J. Sander, "Rain Attenuation of Millimeter Waves at wavelength = 5.77, 3.3 and 2 mm," *IEEE Transactions on Antennas and Propagation*, vol. 23, pp. 213-220, March 1975.

[7] R.A. Bohlander et al., "Fluctuations in millimeter-wave signals propagated through inclement weather," *IEEE Transactions on Geoscience and Remote Sensing*, vol. 26, no. 3, pp. 343-354, May 1988.

[8] J. Nemarich, R. J. Wellman, and J. Lacombe, "Backscatter and attenuation by falling snow and rain at 96, 140, and 225 GHz," *IEEE Tranactions on Geoscience and Remote Sensing*, vol. 26, no. 3, pp. 319-329, May 1988.

[9] K. Aydin and Y-M Lure, "Millimeter Wave scattering and propagation in rain: A computational study at 94 and 140 GHz for oblate spheroidal and spherical raindrops," *IEEE TGRS*, vol. 29, no. 4, pp. 593-602, July 1991.

[10] K. Aydin and S. E. A. Daisley, "Relationships between rainfall rate and 35-GHz attenuation and differential attenuation: Modeling the effects of raindrop size distribution, canting, and oscillation," *IEEE TGRS,* vol. 40, no. 11, pp. 2343-2352, Nov. 2002.

[11] H. B. Wallace, "Analysis of RF imaging applications at frequencies over 100 GHz," *Applied Optics*, vol. 49, no. 19, pp. E39-E47, July 2010.

[12] Rajasri Sen and M.P. Singh, "Estimation of cross polarization of millimeter waves due to rain over few stations in India and its modification incorporating measured values of rain height.," in *Antennas and propagation and EM theory, 2003. Proceedings, 2003 6th International Symposium on*, 2003, pp. 568-571.